

Electrochemical Studies on the Corrosion Behaviour of Reinforcing Steel in the Presence of Cyanoacetamide Derivatives as Corrosion Inhibitors

W. M. Yousef^{1,*}, Y. Reda² and A. M. Eldesoky³

¹ Chemistry Department, Faculty of Science, Hail University/ Hail, P. O.Box 2440, Kingdom of Saudi Arabia.

² Chemical Engineering Department, High Institute of Engineering & Technology (New Damietta), Egypt.

³ Engineering Chemistry Department, High Institute of Engineering & Technology (New Damietta), Egypt and Al-Qunfudah Center for Scientific Research (QCSR), Chemistry Department, Al-Qunfudah University College, Umm Al-Qura University, KSA.

*E-mail: wafaa_youssef95@hotmail.com

Received: 24 October 2017 / Accepted: 20 October 2018 / Published: 5 November 2018

Using techniques such as Tafel polarization, (EIS) electrochemical impedance spectroscopy and (EFM) electrochemical frequency modulation, this work explored reinforcing steel corrosion and its inhibition by cyanoacetamide derivatives in 2 M HCl solutions. As indicated by the electrochemical analysis, a reduced corrosion rate and corrosion current density as well as more positive corrosion potential values were obtained by adding and increasing the concentration of the cyanoacetamide derivatives. The orders of the inhibition efficiency (% η) of Cyanoacetamide derivatives are given: (1) > (2) > (3). Molecular docking was used to predict the binding between Cyanoacetamide derivatives with the receptor of 3tt8-hormone of crystal structure analysis of Cu Human Insulin Derivative.

Keywords: Reinforcing Steel, Cyanoacetamide, EIS, EFM, , Molecular docking

1. INTRODUCTION

Reinforcing steel is among the most frequently used construction materials for strengthening concrete structures and therefore makes a remarkable contribution to the development of the economy. Nevertheless, on a global scale, the corrosion of reinforcing steel is an important issue because it is a main cause of the premature degradation of concrete structures [1-3]. Thus, there is an urgent need for contemporary research on the mechanisms of corrosion as well as on the protection of steel. Typically, a passive film is generated on the surface of steel within concrete pore solutions that typically have a

significantly alkaline pH of 12.0 to 13.0, thus inhibiting the corrosion of the reinforcing steel in concrete. It is believed that the passive oxide film is thin with a certain adherence and that it inhibits corrosion through the generation of an Fe_2O_3 layer on the surface [4]. Nevertheless, both the chemical and physical conditions at the interface between the media and the steel determine whether the passivity of the steel lasts. When the critical chloride concentration and/or pH value for corrosion at the interface between the concrete and steel is achieved, the reinforcing steel will corrode due to damage of the protective film [5-11].

A popular hypothesis is that the dissolution of metals can be prevented via eliminating the unfavourable and destructive effects of the aggressive media through the use of corrosion inhibitors. Most of the inhibition occurs when the inhibitor adsorbs onto and interacts with the surface of the iron [12-14]. In addition to the adsorption mechanism, the relations between the adsorption traits and the various forms of organic corrosion inhibitors are also a consideration for researchers. Polymeric complexes can be generated on the surfaces of metals, in which azole derivatives, such as benzimidazole, benzotriazole, imidazole, and mercaptobenzothiazole, all popular corrosion inhibitors, are adsorbed onto the surface. Conversely, a protective film can also be adhered onto a metal and obstruct interactions with aggressive ions such as chloride [15]. Based on previous literature, heterocyclic compounds containing conjugated double bonds and polar functional groups generally exhibit good inhibition performance, as do organic compounds with polar groups, including nitrogen, oxygen, phosphorus, and sulfur [16-20]. Such organic compounds interact with the surface of the metal where they are adsorbed, which accounts for most of the inhibition. Stable adsorption is concentrated at the functional polar groups, which are known as the centers of the reaction. Nevertheless, on the surface of a metal, several factors, including the chemical structure of the protective inhibitor, surface charge of the metal, traits of the metal, type of electrolyte solution, and mode of adsorption, determine the inhibitor adsorption.

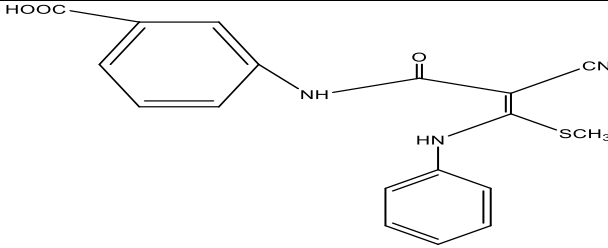
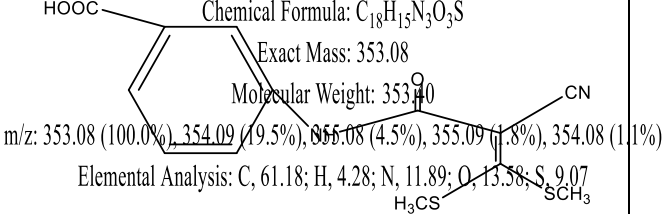
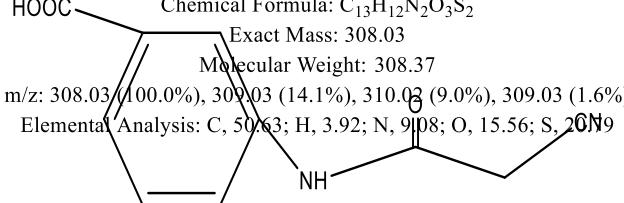
The point of this work is to study Inhibiting effect of some cyanoacetamide derivatives (1-3) on the corrosion behavior of reinforcing steel in 2 M HCl solution using various electrochemical techniques. Molecular docking was used to predict the binding between Cyanoacetamide derivatives (1-3) with the receptor of 3tt8-hormone of crystal structure analysis of Cu Human Insulin Derivative.

2. EXPERIMENTS

2.1. Materials

R235 reinforcing steel containing C (0.390), Cu (0.101) Mn (0.254), Ni (0.027), P (0.015), S (0.012), Si (0.083) (wt. %) and the balance of Fe was designated as the target material. Cyanoacetamide derivatives (1-3) studied in this work have the structures and molecular weights listed in Table.1. Appropriate concentration of Hydrochloric acid was prepared by using bidistilled water. 1×10^{-3} M stock solutions from the investigated Cyanoacetamide derivatives (1-3) were prepared by dissolving the appropriate weights of the used chemically pure solid compounds in absolute ethanol [21].

Table 1. Structure and molecular weights of the studied Cyanoacetamide derivatives (1-3).

Cpd. No.	Structures and Names	Formulas& Molecular Weights
(1)	 <p>(E)-3-(2-cyano-3-(methylthio)-3-(phenylamino)acrylamido)benzoic acid</p>	$C_{18}H_{15}N_3O_3S$ 353.08
(2)	 <p>Chemical Formula: $C_{13}H_{12}N_2O_3S_2$ Exact Mass: 353.08 Molecular Weight: 353.40 m/z: 353.08 (100.0%), 354.09 (19.5%), 355.08 (4.5%), 355.09 (1.8%), 354.08 (1.1%) Elemental Analysis: C, 61.18; H, 4.28; N, 11.89; O, 13.58; S, 9.07</p> <p>3-(2-cyano-3,3-bis(methylthio)acrylamido)benzoic acid</p>	$C_{13}H_{12}N_2O_3S_2$ 308.37
(3)	 <p>Chemical Formula: $C_{10}H_8N_2O_3$ Exact Mass: 308.03 Molecular Weight: 308.37 m/z: 308.03 (100.0%), 309.03 (14.1%), 310.03 (9.0%), 309.03 (1.6%) Elemental Analysis: C, 50.63; H, 3.92; N, 9.08; O, 15.56; S, 20.19</p> <p>3-(2-cyanoacetamido)benzoic acid</p>	$C_{10}H_8N_2O_3$ 204.19

2.2. Electrochemical measurements

2.2.1. Potentiodynamic polarization technique

Elemental Analysis: C, 58.82; H, 3.95; N, 13.72; O, 23.51

Potentiodynamic measurements were performed using an ordinary three-compartment glass cell of a capacity 100 ml that contain three different types of electrodes; R235 reinforcing steel specimen as working electrode, saturated calomel electrode (SCE) as a reference electrode, and a platinum foil as an auxiliary electrode. The working electrode was embedded in a Teflon rod with an exposed area of 1 cm². This electrode was immersed in 100 ml of a test solution into the polarization cell. A time interval of about 30 minutes was given for the system to attain a steady state [open-circuit potential (E_{ocp})]. All the experiments were carried out at 25 ± 0.1 °C by using an ultra-circulating thermostat. The Potentiodynamic current potential curves were recorded by changing the electrode potential automatically from -0.8 to 0.8 mV versus open circuit potential (E_{ocp}) with a scan rate of 1 mV/s.

2.2.2. EFM and EIS techniques

Electrochemical tests were lead to three electrodes cell thermostatic utilized a Gamrypotentiostat/galvanostat/ZRA (model PCI300/4). A saturated calomel and platinum electrode

were utilized as reference and auxiliary electrodes. The R235 reinforcing steel electrodes were 10x10 ml and were welded with a copper wire on one side. All method were done at temperature (25 ± 0.1 °C). The potentiodynamic diagrams were measured from -50 to 50 V at a rate scan 1 mV S^{-1} after the steady state is approached (30 min) and the open potential circuit was observed after putted the electrode for 15 min in the solution test.

(EFM) and (EIS) tests were obtain by utilized the same methods as before with a Gamry framework system depend on ESA400. EchemAnalyst 5.5 Software was utilized for drawing, graphing and fitting data. EIS tests were done in a range of frequency of 100 kHz to 10 mHz with amplitude of 5 mV peak-to-peak ac signals utilized at respective for potential corrosion. EFM had done utilized 2 frequencies 2 and 5 Hz. The frequency base was 1 Hz. In this research, we utilized a signal perturbation with amplitude of 10 mV for both frequencies perturbation of 2 and 5 Hz.

2.3. Measurements

This study mimics the real docking process in which the ligand–protein pair-wise interaction energies are calculated using Docking Server [22]. The MMFF94 Force field was for used energy minimization of ligand molecule using Docking Server. Gasteiger partial charges were added to the ligand atoms. Non-polar hydrogen atoms were merged, and rotatable bonds were defined. Docking calculations were carried out on Cyanoacetamide derivatives (1-3) protein model. Essential hydrogen atoms, Kollman united atom type charges, and solvation parameters were added with the aid of AutoDock tools [23]. Affinity (grid) maps of $20 \times 20 \times 20 \text{ \AA}$ grid points and 0.375 \AA spacing were generated using the Autogrid program [24]. AutoDock parameter set- and distance-dependent dielectric functions were used in the calculation of the van derWaals and the electrostatic terms, respectively.

3. RESULTS AND DISCUSSION

3.1. Potentiodynamic polarization measurements

Polarization measurements were carried out to obtain Tafel plots in the absence and presence of various concentrations of the investigated derivatives. Figure.(1), shows the current-potential relationship for the R235 reinforcing steel electrode at different test solutions of compound (1) [as the most effective inhibitor], similar curves were obtained for the other compounds (not shown). The corrosion kinetic parameters such as corrosion current density (i_{corr}), corrosion potential (E_{corr}), the anodic Tafel slopes (β_a), cathodic Tafel slope (β_c), degree of surface coverage (θ) and the inhibition efficiency ($\% \eta$) for R235 reinforcing steel in 2 M HCl solution in the absence and presence of different concentrations of all inhibitors are listed in Table 2.

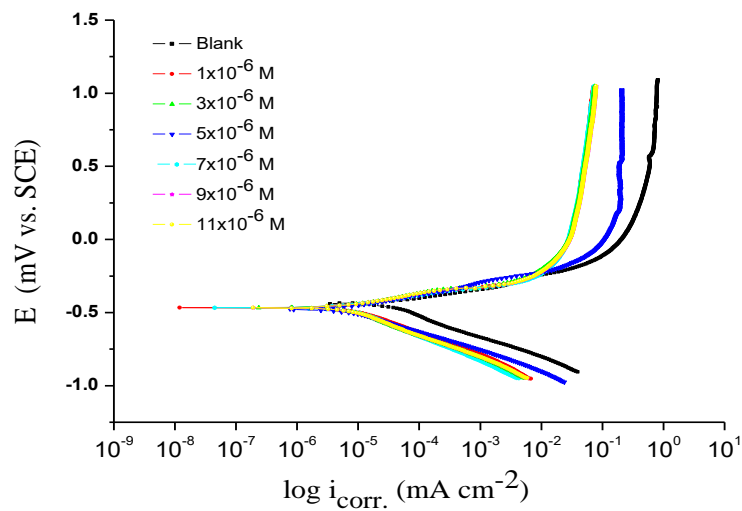


Figure 1. Potentiodynamic polarization diagram for the corrosion of R235 reinforcing steel in 2 M HCl in the absence and presence of various concentrations of compound (1) at 25 ± 0.1 °C.

Table 2. Corrosion kinetic parameters for R235 reinforcing steel in 2 M HCl solution in the absence and presence of different concentrations of all inhibitors at 25 ± 0.1 °C.

Cpd. No.	Conc.,M.	$-E_{\text{corr}}$ (mV vs. SCE)	$i_{\text{corr}} \times 10^{-5}$ ($\mu\text{A cm}^{-2}$)	$\beta_{\text{ax}} \times 10^{-3}$ (mV dec $^{-1}$)	$\beta_{\text{cx}} \times 10^{-3}$ (mV dec $^{-1}$)	θ	% η
	Blank	439	45.30	81.60	234.0	----	-----
(1)	1×10^{-6}	477	8.82	88.90	166.8	0.805	80.5
	3×10^{-6}	467	8.77	91.70	214.5	0.806	80.6
	5×10^{-6}	478	8.55	100.20	158.1	0.811	81.1
	7×10^{-6}	489	8.46	83.60	188.1	0.813	81.3
	9×10^{-6}	482	2.83	49.40	91.7	0.937	93.7
	11×10^{-6}	466	1.78	36.70	63.9	0.960	96.0
(2)	1×10^{-6}	479	10.00	81.90	166.8	0.779	77.9
	3×10^{-6}	454	9.90	71.80	147.7	0.781	78.1
	5×10^{-6}	466	9.77	79.80	152.5	0.784	78.4
	7×10^{-6}	467	9.45	96.50	237.4	0.791	79.1
	9×10^{-6}	468	9.19	91.20	175.2	0.797	79.7
	11×10^{-6}	466	9.07	88.00	204.8	0.799	79.9
(3)	1×10^{-6}	439	42.70	78.10	215.4	0.057	5.7
	3×10^{-6}	467	22.50	113.50	232.2	0.503	50.3
	5×10^{-6}	453	17.40	74.30	158.2	0.615	61.5
	7×10^{-6}	479	11.00	89.00	152.7	0.757	75.7
	9×10^{-6}	467	10.70	79.70	147.1	0.763	76.3
	11×10^{-6}	480	10.50	106.40	155.4	0.768	76.8

These tabulated data indicated that, the presence of these derivatives shifts both anodic and cathodic branches to the lower values of corrosion current densities (i_{corr}) and thus causes a remarkable decrease in the corrosion rate, this implies that both the hydrogen evolution and the anodic dissolution of R235 reinforcing steel are inhibited as a result of the adsorption of the inhibitors on the corroding surface [25,26]. The Tafel slopes of β_a and β_c at 25 ± 0.1 °C do not change remarkably upon addition of inhibitors, which indicates that the presence of these additives does not change the mechanism of hydrogen evolution and the metal alloy dissolution process, and that inhibitors affects both anodic and cathodic reactions [27], i.e. it is mixed type inhibitors. Inhibition efficiency (% η) and degree of surface coverage (θ) were calculated using the following Eq. (1):

$$\% \eta = \theta \times 100 = [1 - (i_{\text{corr}} / i_{\text{corr}}^0)] \times 100 \quad (1)$$

where (i_{corr} and i_{corr}^0) are the corrosion current densities in the presence and absence of inhibitors, respectively. The order of % η was found to decrease in the following sequence: (1) > (2) > (3).

3.2. (EIS) tests

EIS measurements were carried out at 25 ± 0.1 °C in acid solution with and without inhibitors. The equivalent circuit model which describes the metal / electrolyte interface of the present corroding system is shown as insert in Figure. (2), where R_s , R_{ct} and CPE refer to solution resistance, charge transfer resistance and constant phase element representing the double layer capacitance (C_{dl}) of the interface, respectively. A typical example of EIS data obtained for compound (1) [as the most effective inhibitor] is represented as Bode and Nyquist plots in Figures. (3a and 3b). Similar curves were obtained for other compounds (not shown). The impedance spectra consists of a Nyquist semicircle type without appearance of diffusive contribution to the total impedance (Z) indicating that the corrosion proceeds mainly under charge-transfer control [28] and the presence of inhibitor do not alter the mechanism of corrosion reaction. Small distortion was observed in the diagrams, this distortion has been attributed to frequency dispersion [29]. The obtained diameters of the capacitive loops increase in presence of inhibitors, and are indicative of the extent of inhibition of corrosion process, contrary to the decrease of the capacity of double layer (C_{dl}) which is defined from Eq. (2):

$$C_{\text{dl}} = (2 \pi f_{\text{max}} R_{\text{ct}})^{-1} \quad (2)$$

where $Y_o = \text{CPE magnitude}$, $\omega = 2\pi f_{\text{max}}$, f_{max} = the imaginary frequency at which the component of the impedance is maximal.

The inhibition efficiencies obtained from the EIS measurements are calculated from Eq. (3):

$$\% \eta = \theta \times 100 = [1 - (R_{\text{ct}}^0 / R_{\text{ct}})] \times 100 \quad (3)$$

where R_{ct}^0 and R_{ct} are the charge-transfer resistance values without and with inhibitor, consecutively.

The analysis of the EIS parameters shows that the diameters of the semicircle increases with increasing the concentration of the investigated inhibitors. This indicates that the polarization resistance R_{ct} of the oxide layer increases with increasing the concentration of inhibitors, giving consequently a decrease in the corrosion rate. The depressed capacitive semicircles are often referred to the surface roughness and inhomogeneity, since this capacitive semicircle is correlated with

dielectric properties and thickness of the barrier oxide film. It is important to ensure that the values of C_{dl} decrease with increasing the inhibitor concentration, this is due to the gradual replacement of water molecules in the double layer by the adsorbed inhibitor molecules which form an adherent film on the metal surface and leads to decrease in the local dielectric constant of the metal solution interface [30]. The high frequency limits corresponds to $(R_{ct} + R_s)$. The low frequency contribution shows the kinetic response of charge transfer reaction [31]. EIS data are shown in Table .(3), from this Table, it is clear that the inhibition efficiency (% η) of these compounds follows the same sequence as before: (1) > (2) > (3).

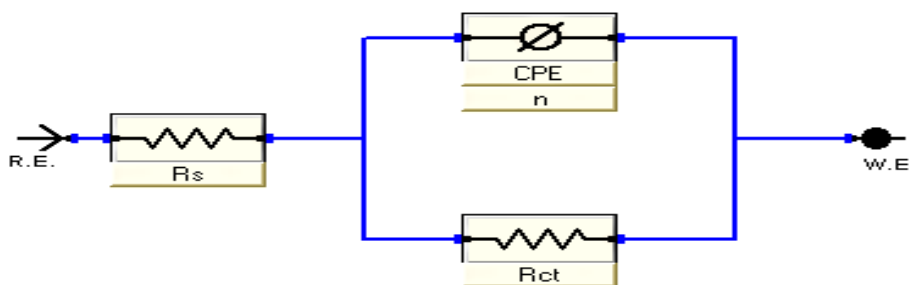


Figure 2. Circuit equivalent utilized to fit EIS data.

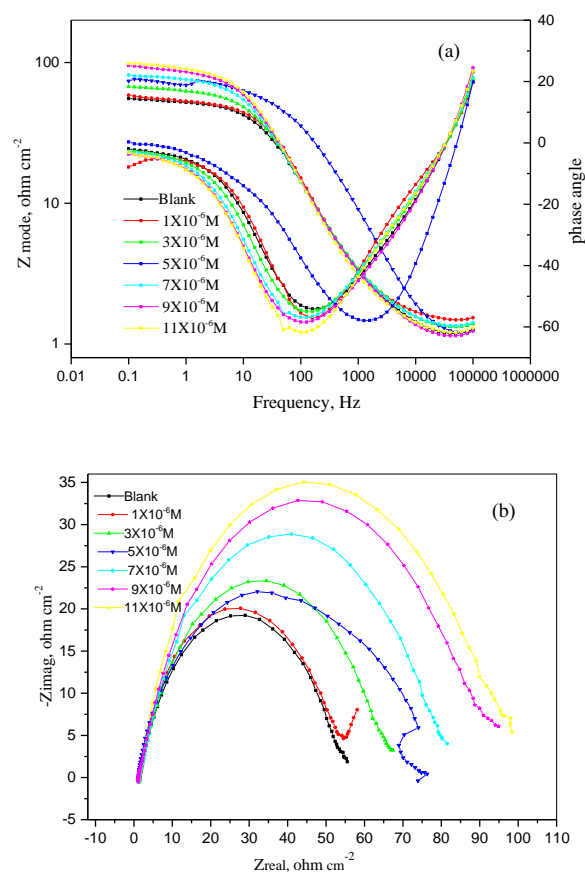


Figure 3. EIS Bode plots (a) and Nyquist plots (b) for the corrosion of R235 reinforcing steel in 2 M HCl in the absence and presence of various concentrations of compound (1) at 25 ± 0.1 °C.

Table 3. kinetic parameters given by EIS test for R235 reinforcing steel in 2 M HCl in the absence and presence of various concentrations of Cyanoacetamide derivatives at 25 ± 0.1 °C.

Cpd. No.	Conc., M.	R_s ($\Omega \text{ cm}^2$)	$Y_o \times 10^{-6}$	$n \times 10^{-3}$	R_{ct} ($\Omega \text{ cm}^2$)	$C_{dl} \times 10^{-4}$ (μFcm^{-2})	θ	% η
	Blank	1.021	116.3	797.4	50.86	2.79	-----	-----
(1)	1×10^{-6}	1.152	444.1	775.3	97.02	1.99	0.475	47.5
	3×10^{-6}	1.351	446.2	774.2	97.72	1.31	0.479	47.9
	5×10^{-6}	1.291	469.4	762.3	112.02	1.23	0.545	54.5
	7×10^{-6}	1.197	457.9	771.4	131.10	1.11	0.612	61.2
	9×10^{-6}	1.351	451.2	769.8	164.90	1.06	0.691	69.1
	11×10^{-6}	1.381	448.2	782.3	192.90	1.01	0.736	73.6
(2)	1×10^{-6}	1.282	333.6	813.4	58.90	2.01	0.136	13.6
	3×10^{-6}	1.571	361.1	819.6	66.74	1.34	0.237	23.7
	5×10^{-6}	1.493	382.0	802.9	70.41	1.21	0.277	27.7
	7×10^{-6}	1.821	423.4	796.7	89.92	1.16	0.434	43.4
	9×10^{-6}	2.199	445.1	773.4	93.06	1.13	0.453	45.3
	11×10^{-6}	2.462	446.1	775.3	100.09	1.04	0.491	49.1
(3)	1×10^{-6}	1.621	343.7	889.4	57.41	2.06	0.114	11.4
	3×10^{-6}	1.721	221.2	891.3	61.12	1.35	0.167	16.7
	5×10^{-6}	1.236	305.4	896.2	67.02	1.26	0.241	24.1
	7×10^{-6}	1.068	391.8	863.4	71.23	1.17	0.285	28.5
	9×10^{-6}	1.042	259.4	891.4	85.93	1.15	0.408	40.8
	11×10^{-6}	1.168	113.4	871.5	98.93	1.06	0.485	48.5

3.3. EFM method

The EFM is a safe and accurate corrosion measurement technique that can directly determine the corrosion current without prior knowledge of Tafel constants and with only a small polarizing

signal. These advantages of EFM technique make it an ideal and non-destructive candidate for corrosion monitoring [32]. Intermodulation spectra obtained from EFM measurements are presented in Figure.(4) as example of R235 reinforcing steel in corroded 2 M HCl solutions without and with various concentrations of compound (1) [as the most effective inhibitor] at 25 ± 0.1 °C. Similar intermodulation spectra were obtained for other compounds (not shown). Each spectrum is a current response as a function of frequency. The calculated corrosion kinetic parameters at different concentrations of the investigated compounds in 2 M HCl at 25 ± 0.1 °C. (i_{corr} , β_a , β_c , CF-2, CF-3 and $\% \eta$) are given in Table.(4). From Table 4, the corrosion current densities decreased by increasing the concentration of investigated inhibitors and so the inhibition efficiencies increased. The causality factors in Table.(4) are very close to the theoretical values which according to EFM theory [33] that guarantee the validity of Tafel slopes and corrosion current densities, they also indicate that the measured data are of good quality. The standard values for CF-2 and CF-3 are 2.0 and 3.0, respectively. The deviation of causality factors from their ideal values may occur due to the smaller perturbation amplitude or due to the resolution of the frequency spectrum is not high enough, also another possible explanation that the inhibitor is not performing very well. The obtained results showed good agreement of corrosion kinetic parameters obtained with the EIS and Tafel polarization measurements.

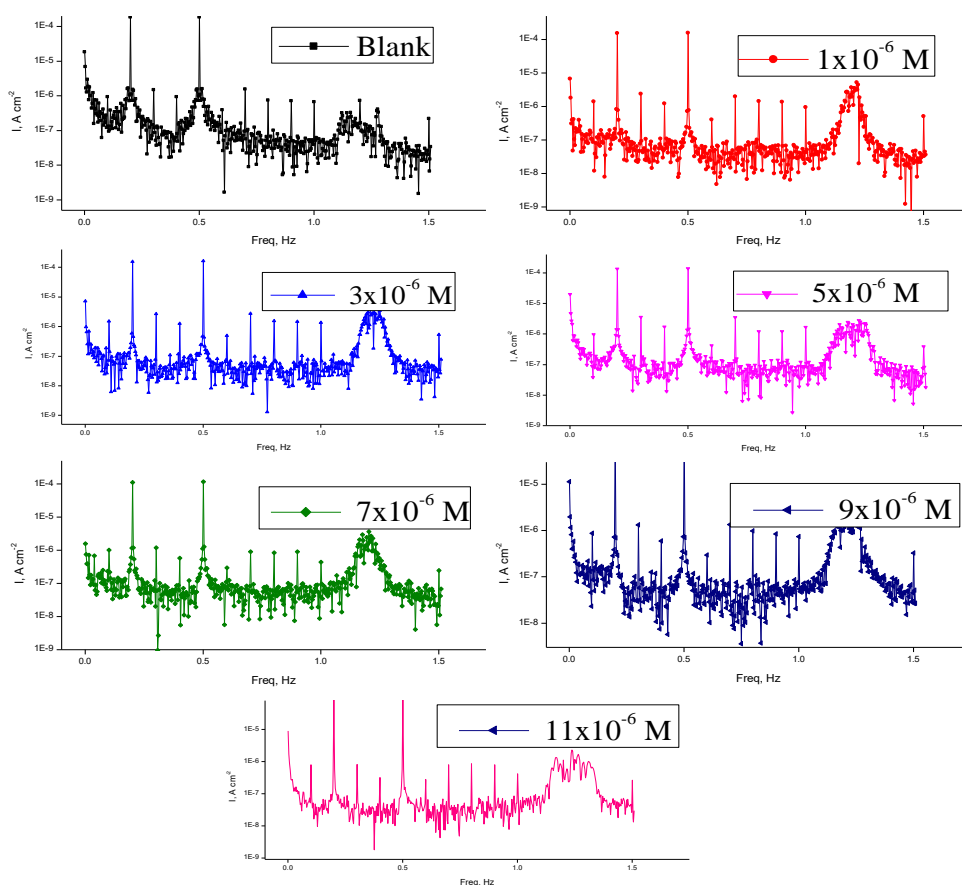


Figure 4. EFM spectra for the corrosion of R235 reinforcing steel in 2 M HCl in the absence and presence of various concentrations of compound (1) at 25 ± 0.1 °C.

Table 4. Electrochemical kinetic parameters obtained by EFM technique for R235 reinforcing steel in 2 M HCl in the absence and presence of various concentrations of Cyanoacetamide derivatives at 25 ± 0.1 °C.

Cpd. No.	Conc., M.	i_{corr} ($\mu\text{A cm}^{-2}$)	$\beta_a \times 10^{-3}$ (mV dec^{-1})	$\beta_c \times 10^{-3}$ (mV dec^{-1})	CF-2	CF-3	θ	% η
	Blank	509.1	172.3	189.3	1.93	2.87	----	----
(1)	1×10^{-6}	264.2	101.4	118.7	2.02	3.04	0.481	48.1
	3×10^{-6}	263.4	113.2	113.4	2.01	3.05	0.482	48.2
	5×10^{-6}	249.8	117.1	120.2	2.10	3.06	0.509	50.9
	7×10^{-6}	223.2	109.6	123.4	2.06	2.96	0.561	56.1
	9×10^{-6}	113.2	119.7	119.8	2.03	3.03	0.777	77.7
	11×10^{-6}	97.4	121.2	125.6	1.99	3.01	0.808	80.8
(2)	1×10^{-6}	294.1	121.6	118.1	1.89	3.04	0.422	42.2
	3×10^{-6}	273.6	118.7	122.8	2.03	2.99	0.462	46.2
	5×10^{-6}	251.3	121.7	110.4	1.97	2.96	0.506	50.6
	7×10^{-6}	233.4	109.6	114.8	1.94	2.89	0.541	54.1
	9×10^{-6}	119.6	123.9	120.3	2.06	2.98	0.765	76.5
	11×10^{-6}	102.3	126.7	121.2	2.09	3.07	0.799	79.9
(3)	1×10^{-6}	301.6	114.0	1.98	3.01	2.96	0.407	40.7
	3×10^{-6}	289.6	107.8	2.01	2.03	3.01	0.431	43.1
	5×10^{-6}	264.7	105.6	2.00	2.99	3.03	0.480	48.0
	7×10^{-6}	244.6	123.2	1.96	2.97	2.99	0.519	51.9
	9×10^{-6}	125.7	117.9	2.01	1.87	2.98	0.751	75.1
	11×10^{-6}	109.6	121.2	1.97	1.99	2.89	0.784	78.4

3.4. Molecular docking

The docking study showed a favorable interaction between Cyanoacetamide derivatives (1-3) and the receptor of 3tt8-hormone of crystal structure analysis of Cu Human Insulin Derivative. The calculated energy is listed in Table 5 and Figure.(5) .

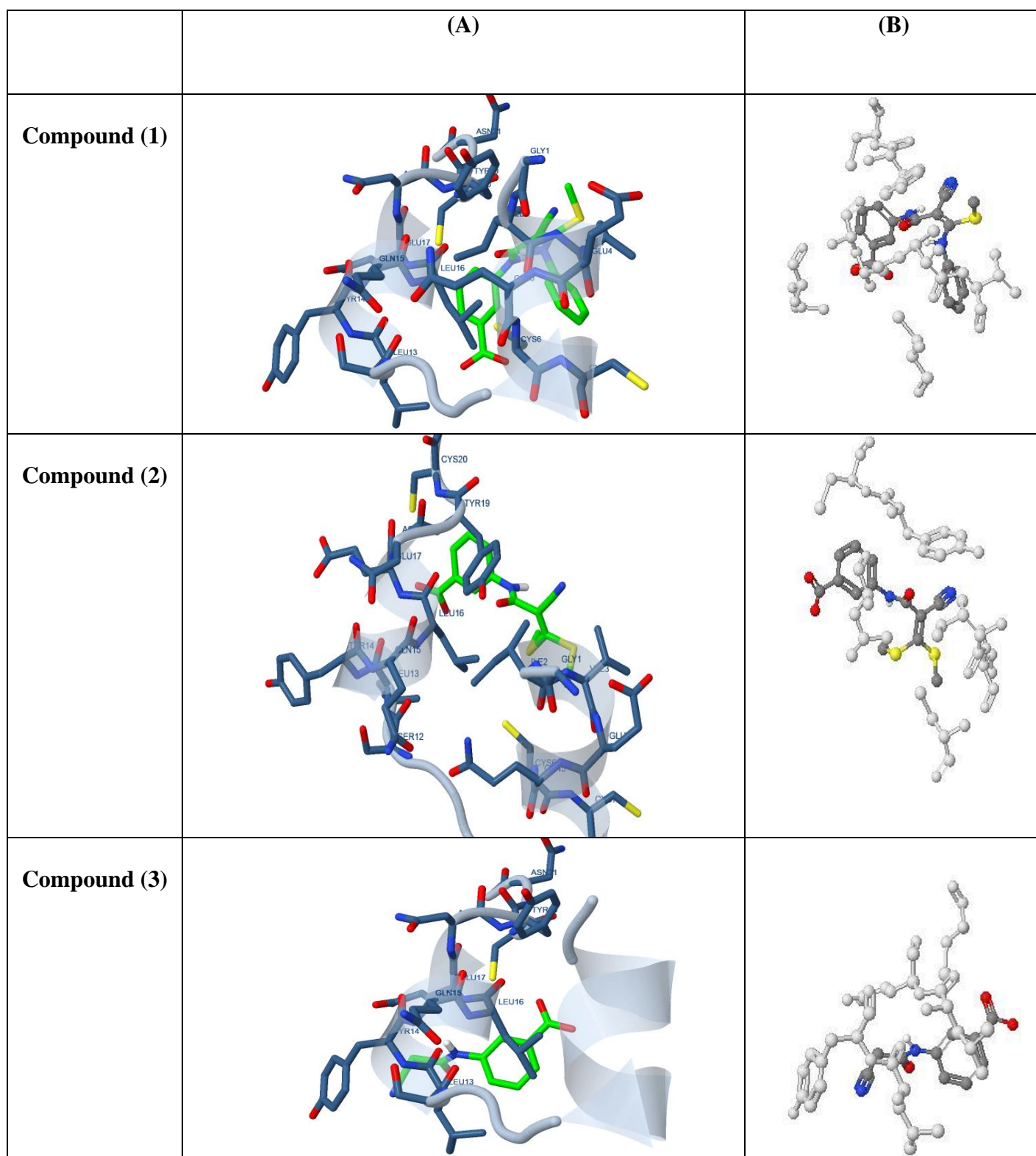


Figure 5. Cyanoacetamide derivatives (1-3) (green in (A) and gray in (B)) in interaction with 3tt8 receptor. (For interpretation of the references to color in this figure legend, the reader is referred to the web version of this article).

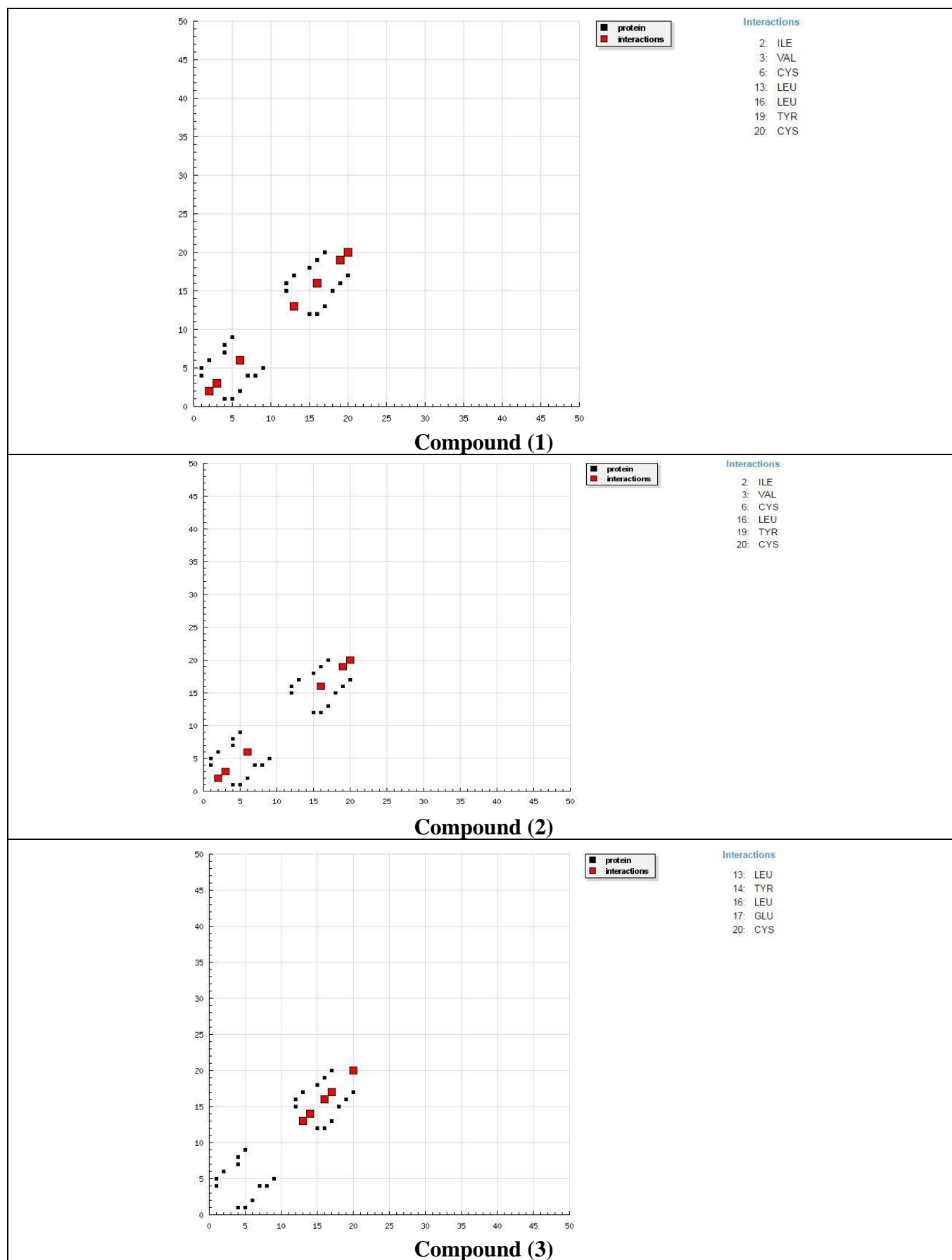
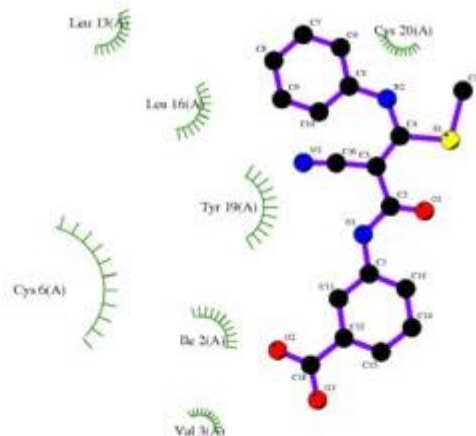


Figure 6. HB plot of interaction between Cyanoacetamide derivatives (1-3) with receptor of breast cancer mutant 3tt8.

Compound (1)



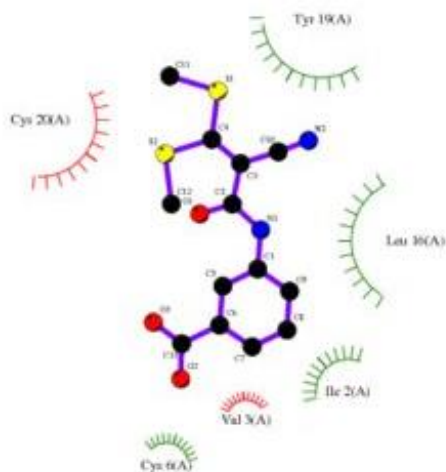
Key

- ● Ligand bond
- ● Non-ligand bond
- ● Hydrogen bond and its length

Res. 55 Non-ligand residues involved in other contact(s)

docking

Compound (2)



Key

- ● Ligand bond
- ● Non-ligand bond
- ● Hydrogen bond and its length

Res. 55 Non-ligand residues involved in other contact(s)

docking

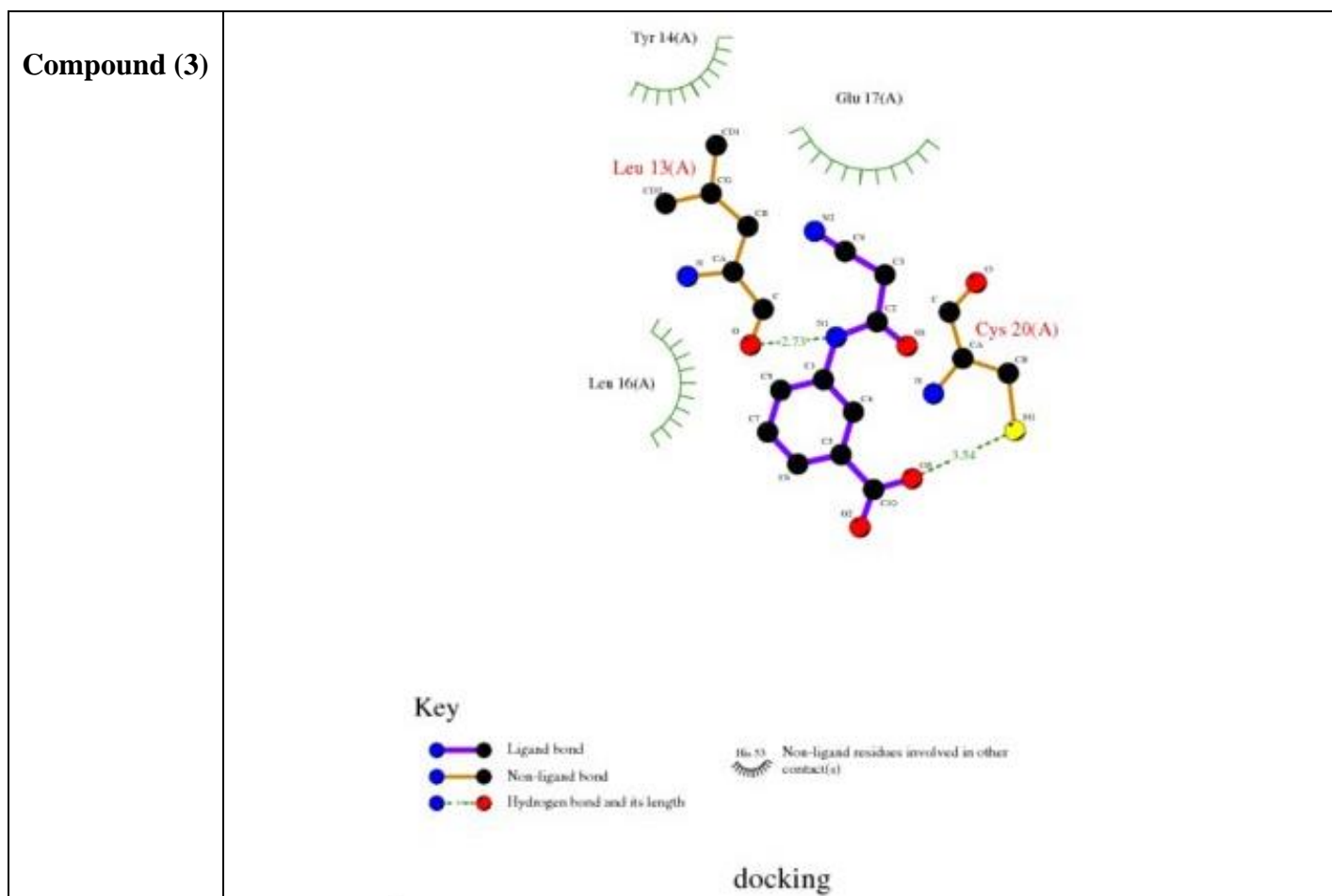


Figure 7. 2D plot of interaction between Cyanoacetamide derivatives (1-3) with 3tt8 receptor.

Table 5. Energy values obtained in docking calculations of Cyanoacetamide derivatives (1-3) with 3tt8 receptor.

Cpd. No.	Estimating free energy of binding (kcal/mol)	Estimating inhibition constant (K_i) (μ M)	Electrostatic Energy (kcal/mol)	Total intercooled Energy (kcal/mol)	Interact surface
(1)	-4.59	429.65	-0.04	-6.50	530.593
(2)	-4.46	536.07	-0.01	-5.73	518.834
(3)	-3.90	1.38	-0.16	-5.00	406.386

According to the results obtained in this study, HB plot curve indicated that, the Cyanoacetamide derivatives (1-3) binds to the proteins hydrogen bond and decomposed interactions energies in kcal/mol were existed between the Cyanoacetamide derivatives (1-3) with 3tt8 receptor as shown in Figure .(6).The calculated efficiency is favorable where K_i values estimated by AutoDock were compared with experimental K_i values, when available, and the Gibbs free energy is negative

[34]. Also, based on this data, it can propose that interaction between the 3tt8 receptor and the Cyanoacetamide derivatives (1-3) is possible. 2D plot curves of docking with Cyanoacetamide derivatives (1-3) are shown in Figure.(7).

3.5. Mechanism of Corrosion protection

Adsorption of organic compounds which is the essential mechanism of corrosion inhibition can be explained by two basic types of interactions: physisorption and chemisorption. Physical adsorption requires the presence of both the electrically charged surface of the metal and charged species in solution. The surface charge of the metal is due to the electric field existing at the metal/solution interface. A chemisorption process, on the other hand, involves charge sharing or charge transfer from the inhibitor molecules to the metal surface to form a coordinate type of a bond. Thus, we can conclude that inhibition of R235 reinforcing steel corrosion in 2 M HCl is mainly due to electrostatic interaction and chemical adsorption. The maximum inhibition efficiency was obtained for R235 reinforcing steel corrosion in 2 M HCl by compound (1) is 91.6% in comparison to Tagetes erecta extract (TEE) (Marigold flower) in 3.5% NaCl solutions was 96% [35]. The order of decreasing inhibition efficiency of the compounds from all techniques used is compound (1) > compound (2) > compound (3) .

Compound (1) exhibits excellent inhibition power due to: (i) it has larger molecular size (353.08) that may facilitate better surface coverage and larger molecular area and (ii) its adsorption through seven active centers (3-O , 3-N and 1- S atoms). Compound (2) comes after compound (1) in inhibition efficiency because it has less molecular size (308.37) and also has seven active centers (3-O , 2-N and 2- S atoms). Compound (3) is the least one in inhibition efficiency, this due to, it has lesser molecular size (204.19), and less active centers (3-O and 2-N atoms).

4. CONCLUSION

All the investigated cyanoacetamide derivatives are good corrosion inhibitors for R235 reinforcing steel in 2 M HCl solution.

Double layer capacitances decrease with respect to blank solution when the inhibitor added. This fact may explained by adsorption of the inhibitor molecule on the R235 reinforcing steel surface .

EFM can be utilized as a fast and nondestructive tests for calculation of corrosion without prior information of Tafel lines.

The data from electrochemical tests were in best agreement. The % η of these compounds investigated is: (1) > (2) > (3).

The % η obtained from polarization curves, electrochemical impedance spectroscopy and electrochemical frequency modulation are in a good agreement.

Molecular docking and binding energy calculations of cyanoacetamide derivatives with the receptor of 3tt8-hormone of crystal structure analysis of Cu Human Insulin Derivative indicated that the compounds are efficient inhibitors of receptor of 3tt8-hormone.

References

1. V. Kumar, *J. Corros. Rev.*, 16 (1998) 317.
2. S. Ahmad, *J. Cem. Concr. Compos.*, 25 (2003) 459.
3. D. Hobbs, *J. Int. Mat. Rev.*, 46 (2001) 117.
4. B. Huet, V. L'Hostis, F. Miserque and H. Idrissi, *J. Electrochim. Acta.*, 51 (2005) 172.
5. Y. Ma, Y. Li and F. Wang, *J. Corros. Sci.*, 51 (2009) 997.
6. K. Ann, J. Ahn and J. Ryou, *J. Const. Build. Mat.*, 23 (2009) 239.
7. M. Montemor, A. Simoes and M. Ferreira, *J. Cem. Concr. Compos.*, 25 (2003) 491.
8. R. Du, R. Hu, R. Huang and C. Lin, *J. Anal. Chem. Lett.*, 78 (2006) 3179.
9. Y. Sun, A. Shieh, S. Kim, S. King, A. Kim, H. Sun and C. Croce, *J. Pharmacol., Biochem. Behav.*, 26 (2016) 2834.
10. S. Joiret, M. Keddou, X.R. Nóvoa, M.C. Pérez, C. Rangel and H. Takenouti, *J. Cem. Concr. Compos.*, 24 (2002) 7.
11. Z. Yao, Y. Sun and C. Kang, *J. Nano LIFE.*, 6 (2016) 1642007.
12. E. Sherif, *J. Appl. Surf. Sci.*, 252 (2006) 865.
13. E. Sherif, R. Erasmus and J. Comins, *J. Electrochimica Acta*, 55 (2010) 3657.
14. E. Sherif and S. Park, *J. Electrochim. Acta*, 51 (2006) 1313.
15. V. Lakshminarayanan, R. Kannan and S. Rajagopalan, *J. Electroanal. Chem.*, 364 (1994) 79.
16. A. Chetouani, A. Aouniti, B. Hammouti, N. Benchat, T. Benhadda and S. Kertit, *Corros. Sci.*, 45 (2003) 1675.
17. P. Zhao, Q. Liang and Y. Li, *J. Appl. Surf. Sci.*, 252 (2005) 1596.
18. J. Yao, B. Ren, Z. Huang, P. Cao, R. Gu and Z. Q. Tian, *J. Electrochimica Acta*, 48 (2003) 1263.
19. M. Bazzaoui, L. Martins, E. Bazzaoui and J. Martins, *Electrochimica Acta*, 47 (2002) 2953.
20. K. Zawada, J. Bukowska, M. Calvo and K. Jackowska, *Electrochimica Acta*, 46 (2001) 2671.
21. W. P. Smith, L. S. Sollis, D. P. Howes, C. P. Cherry, D. I. Starkey and N. K. Cobley, *J. Med. Chem.*, 41 (1998) 787.
22. Z. Bikadi and E. Hazai, *J. Chem. Inf.*, 11 (2009) 1.
23. T. A. Halgren, *J. Comput. Chem.*, 17 (1998) 490.
24. G. M. Morris and D. S. Goodsell, *J. Comput. Chem.*, 19 (1998) 1639.
25. S. A. Umoren, I. B. Obot, E. E. Ebenso, P. C. Okafor, O. Ogboke and E. E. Oguzie, *J. Anti. Corro. Meth. Mat.*, 53 (2006) 277.
26. J. O. M. Bockris and D. Drazic, *Electrochimica Acta*, 7 (1962) 293.
27. A. S. Fouda, A. Al-Sarawy and E. El-Katori, *J. Eur. Chem.*, 1(4) (2010) 312.
28. Li. X. Deng, H. Fu and G. Mu, *Corros. Sci.*, 51 (2009) 620.
29. J. Bessone, C. Mayer, K. Tuttner and W. J. Lorenz, *Electrochim. Acta*, 28 (1983) 171.
30. A. S. Fouda, F. El-Taib. Heikal and M. S. Radwan, *J. Appl. Electrochem.*, 39 (2009) 391.
31. A. S. Fouda, H. A. Mostafa, F. El-Taib. Heikal and G. Y. Elawady, *Corros. Sci.*, 47 (2005) 1988.
32. F. Bentiss, M. Bouanis, B. Mernari, M. Traisnel, H. Vezin and M. Lagrenée, *J. Appl. Surf. Sci.*, 253 (2007) 3696.
33. E. Kus and F. Mansfeld, *Corros. Sci.*, 48 (2006) 965.
34. H. M. Refaat, H. A. El-Badway and Sh. M. Morgan, *J. Mol. Liq.* 220 (2016) 802.
35. L. Zhikun and J. Peng, *Int. J. Electrochem. Sci.*, 12 (2017) 8177.